0026-895X/07/7202-440–449$20.00
MOLECULAR PHARMACOLOGY
Copyright © 2007 The American Society for Pharmacology and Experimental Therapeutics
Mol Pharmacol 72:440–449, 2007

Vol. 72, No. 2
36418/3235287
Printed in U.S.A.

Inhibition of Hypoxia-Induced Increase of Blood-Brain Barrier Permeability by YC-1 through the Antagonism of HIF-1α Accumulation and VEGF Expression

Wei-Lan Yeh, Dah-Yuu Lu, Chun-Jung Lin, Houng-Chi Liou, and Wen-Mei Fu

Department of Pharmacology (W.-L.Y., D.-Y.L., H.-C.L., W.-M.F.) and Graduate Institute of Pharmaceutical Science (C.-J.L.), College of Medicine, National Taiwan University, Taipei, Taiwan

Received March 27, 2007; accepted May 18, 2007

ABSTRACT

Cerebral microvascular endothelial cells form the anatomical basis of the blood-brain barrier (BBB), and the tight junctions of the BBB are critical for maintaining brain homeostasis and low permeability. Ischemia/reperfusion is known to damage the tight junctions of BBB and lead to permeability changes. Here we investigated the protective role of 3-(5′-hydroxymethyl-2′-furyl)-1-benzylindazole (YC-1), against chemical hypoxia and hypoxia/reoxygenation (H/R)-induced BBB hyperpermeability using adult rat brain endothelial cell culture (ARBEC). YC-1 significantly decreased $CoCl_2$- and H/R-induced hyperpermeability of fluorescein isothiocyanate (FITC)-dextran in cell culture inserts. It was found that the decrease and disorganization of tight junction protein zonular occludens-1 (ZO-1) in response to $CoCl_2$, and H/R was antagonized by YC-1. The protection of YC-1 may result from the inhibition of HIF-1α accumulation and production of its downstream target vascular endothelial growth factor (VEGF). VEGF alone significantly increased FITC-dextran permeability and down-regulated mRNA and protein levels of ZO-1 in ARBECs. We further used animal model to examine the effect of YC-1 on BBB permeability after cerebral ischemia/reperfusion. It was found that YC-1 significantly protected the BBB against ischemia/reperfusion-induced injury. Taken together, these results indicate that YC-1 may inhibit HIF-1α accumulation and VEGF production, which in turn protect BBB from injury caused by hypoxia.

Pathological conditions such as tumors, inflammation, and ischemia are known to damage the blood-brain barrier (BBB) and to lead to the increase of permeability and development of vasogenic brain edema, and VEGF is likely to be a candidate to regulate the change of permeability (Schoch et al., 2002). Using in vitro model of the BBB consisting of brain microvascular endothelial cells, hypoxia-induced hyperpermeability is mediated by the VEGF/VEGF receptor system in an autocrine manner (Fischer et al., 1999). Increase of vascular permeability and subsequent inflammatory responses may contribute to pathogenetic cofactors responsible for the development of neurological damage.

This work was supported by research grants from the National Science Council of Taiwan.
Article, publication date, and citation information can be found at http://molpharm.aspetjournals.org.
doi:10.1124/mol.107.036418.

The blood-brain barrier constructed from brain microvessel endothelial cells forms a metabolic and physical barrier to protect the central nervous system from the compositional fluctuations that occur in the blood. The blood-brain barrier, which is different from peripheral microvascular endothelium, is the result of the presence of tight junctions (TJs) between neighboring endothelial cells. Tight junctions are complexes of transmembrane proteins that connect to the cytoarchitecture via membrane-associated accessory proteins. The claudin family and occludin are integral transmembrane proteins. Both of these proteins have multiple transmembrane domains and interact with adjacent cells to form homodimeric bridges (Feldman et al., 2005). Stabilization of TJs involves a network of claudins and occludin-linked to the actin cytoskeleton via the zonular occludens proteins (ZO-1, ZO-2, and ZO-3). ZO proteins are membrane-associated accessory proteins that mediate the linkage between

ABBREVIATIONS: BBB, blood-brain barrier; VEGF, vascular endothelial growth factor; TJ, tight junction; ZO, zonular occludens; bHLH, basic helix-loop-helix; HIF, hypoxia inducible factor; HRE, hypoxia-response element; VEGF, vascular endothelial growth factor; YC-1, 3-(5′-hydroxymethyl-2′-furyl)-1-benzylindazole; sGC, soluble guanylate cyclase; ARBEC, adult rat brain endothelial cell; FITC, fluorescein isothiocyanate; PBS, phosphate-buffered saline; kb, kilobase pair(s); H/R, hypoxia/reoxygenation; PKG, protein kinase G; L-NAME, N^{ω}-nitro-L-arginine methyl ester; 8-Br-cGMP, 8-bromo-cGMP; PCR, polymerase chain reaction; MTT, 3-(4,5-dimethylthiazol-2-yl)-2,5-diphenyltetrazolium; ODQ, 1*H*-[1,2,4]oxadiazolo[4,3-a]quinoxalin-1-one; KT5823, 9-methoxy-9-methoxycarbonyl-8-methyl-2,3,9,10-tetrahydro-8,11-epxoy-1*H*,8*H*,11*H*-2,7*b*-11*a*-triazadibenzo(*a*,*g*)cycloocta(*cde*)-trinden-1-one; TGF-β, transforming growth factor β; ELISA, enzyme-linked immunosorbent assay.

actin and the cytoplasmic tail of claudins and occludin (Gloor et al., 2001). Moreover, ZO proteins are members of membrane-associated guanylate kinase family conserved guanylate kinase domain, an SH3 domain and multiple PDZ domains, suggesting that ZO proteins may participate in signal transduction cascade (González-Mariscal et al., 2000).

HIF-1 is a heterodimer composed of two subunits—HIF-1α (120kDa) and HIF-1β (91–94kDa)—that are basic helix-loop-helix protein of the PAS [PER/ARNT/SIM (periodicity/aryl hydrocarbon receptor nuclear translocator/simple-minded)] family (Wang et al., 1995). HIF-1α is ubiquitinated by von Hippel-Lindau protein and subjected to proteasomal degradation in nonhypoxic cells, whereas HIF-1β is expressed constitutively in all cells (Salceda and Caro, 1997). Exposure of cells to hypoxia or transition metals like cobalt and iron chelators induces HIF-1α expression and inhibits HIF-1α ubiquitination by dissociating von Hippel-Lindau protein from HIF-1α. HIF-1α comprises a bHLH domain near the amino (N) terminal, which is essential for DNA binding to hypoxia-response elements (HREs) in the HIF target genes such as vascular endothelial growth factor (VEGF), endothelin-1, and erythropoietin (Sharp and Bernaudin, 2004).

VEGF, also named vascular permeability factor, is one of the most well known HIF target genex involved in vascular biology (Forsythe et al., 1996). Effects of VEGF on the endothelial cells are evidently mediated by the high-affinity cell surface receptors VEGFR-1 and VEGFR-2. Thus, endothelial cells have a unique and specific spectrum of responses to VEGF (Connolly, 1991). Although many recent reports focused on the angiogenic effect of VEGF, VEGF was initially discovered as a tumor-secreted factor that increases vascular permeability (Senger et al., 1983). During vascular sprouting, cell junctions are partially disorganized, which allows endothelial cells to migrate and proliferate and also increases vascular permeability (Dvorak et al., 1995; Dejana, 2004).

YC-, was first introduced to increase NO-soluble guanylate cyclase (sGC) activity and cGMP level on platelets (Ko et al., 1994). However, YC-1-mediated responses via cGMP-independent pathway have also been reported (Hsu et al., 2003; Chien et al., 2005). In addition, growing evidence suggests that YC-1 exerts a novel inhibitory effect on the accumulation of HIF-1α, which in turn blocks the expression of VEGF and antiangiogenesis (Yeo et al., 2003, 2004). Here, we examined whether YC-1 inhibits the destruction and hyperpermeability of BBB induced by cobalt, hypoxia/reoxygenation, or ischemia/reperfusion. We demonstrated that YC-1 significantly inhibits HIF-1α accumulation and VEGF production caused by hypoxia treatment in ARBECs. The in vivo study also reveals that YC-1 is able to protect BBB from ischemia/reperfusion-induced injury.

Materials and Methods

Materials. YC-1 was provided by Yung-Shin Pharmaceutical Industry Co. Ltd. (Taichung, Taiwan). Dimethyl sulfoxide served as vehicle and was purchased from Sigma (St. Louis, MO). $CoCl_2$, a hypoxia mimetic agent, was purchased from Wako Pure Chemicals (Tokyo, Japan). Recombinant human VEGF, goat anti-rat VEGF antibody, and goat control IgG antibody were purchased from R&D Systems (Minneapolis, MN).

Cell Cultures. Immortalized adult rat brain endothelial cells (ARBECs) were a generous gift from National Research Council of Canada (Garberg et al., 2005). ARBECs were seeded onto 75-cm^2 flasks coated with type I rat tail collagen (50 μg/ml; Sigma, St. Louis, MO) and maintained in M199 (Invitrogen, Carlsbad, CA) containing 1% D-glucose solution, 1% Eagle's basal medium amino acid solution, 1% Eagle's basal medium vitamin solution (Sigma), 100 U/ml penicillin, 100 mg/ml streptomycin, 10% heat-inactivated fetal bovine serum (Hyclone, Logan, UT) at 37°C in a humidified incubator under 5% CO_2 and 95% air. Confluent cultures were passaged by trypsinization. Cells from passage 35~45 were used and starved overnight before experiments.

Hypoxia-Reoxygenation of Cultured ARBECs. To induce hypoxia, confluent monolayers of ARBEC cultures were placed into special chamber (Anaerobic System PROOX model 110; BioSpherix, Redfield, NY), which was closed and placed inside an incubator at 37°C and gassing the special chamber with a gas mixture consisting of 95% N_2/5% CO_2. After 24 h, cell cultures were moved out of the hypoxia chamber and reoxygenated in a regular normoxic incubator (95% air, 5% CO_2) for another 4 h. For comparison, control cultures were incubated under normoxic conditions for the same duration.

Cell Viability Assay. Cell viability was assessed by MTT assay. ARBECs cultured onto 24-well plates coated with type I rat tail collagen were induced chemical hypoxia using $CoCl_2$, or suffered an H/R insult in the presence or absence of YC-1. Culture medium was aspirated 24 h after treatment and MTT (0.5 mg/ml; Sigma) was added in each well. MTT was then removed 30 min later and cells were lysed by DMSO. The absorbance was measured at 550 nm by microplate reader (Bio-Tek, Winooski, VT).

Assay of Paracellular Permeability. The permeability assay using cell culture insert system was performed as described previously (Andriopoulou et al., 1999) with minor modifications. ARBECs 4×10^4 were seeded onto cell culture inserts (diameter, 10 mm; pore size, 0.4 μm; polycarbonate membrane, Nalge Nunc International, Rochester, NY) coated with type I rat tail collagen (50 μg/ml, 100 μl). When cultured cells were confluent, FITC-dextran (1 mg/ml, 500 μl; average molecular mass, 43,200; Sigma) was then added into the upper compartment followed by addition of $CoCl_2$ or putting the culture inserts into hypoxia chamber in the absence or presence of YC-1. At the indicated time points, 50 μl of sample medium was taken from the lower compartment. After a dilution of the sample medium to 500 μl with PBS, fluorescence intensity of FITC-dextran was measured at excitation and emission wavelengths of 492 nm and 520 nm, respectively, by a fluorescent reader (Spectra MAX Gemini XS).

Western Blot Analysis. ARBECs were seeded onto 6-cm dishes coated with type I rat tail collagen. Cells were exposed to drugs for 6 or 24 h for detection of HIF-1α or TJ proteins, respectively. After washing with ice-cold PBS, cells were lysed with radioimmunoprecipitation assay buffer (200 μl/dish) on ice for 30 min. After centrifugation at 18,000g for 20 min, the supernatant was used for Western blotting. Protein concentration was measured by BCA assay kit (Pierce, Rockford, IL) with BSA as a standard. Equal proteins (30 μg for TJ proteins and 80 μg for HIF-1α) were separated on 8% SDS polyacrylamide gels and transferred to polyvinylidene difluoride (PVDF) membranes (Millipore, Billerica, MA). The membranes were incubated for 1 h with 4% dry skim milk in PBS buffer to block nonspecific binding and then incubated with rabbit antibodies against occludin (1:1000; Santa Cruz Biotechnology, Santa Cruz, CA), claudin-1, ZO-1 (1:1000; Zymed, South San Francisco, CA) or mouse antibodies against HIF-1α (1:1000; Novus Biologicals, Littleton, CO), α-tubulin (1:1000; Santa Cruz Biotechnology) for 1 h. After washing with PBS-Tween 20, the membranes were incubated with goat anti-rabbit or anti-mouse peroxidase-conjugated secondary antibody (1:1000; Santa Cruz Biotechnology) for 1 h. The blots were visualized by enhanced chemiluminescence (ECL; Santa Cruz Biotechnology) using Kodak X-OMAT LS film (Eastman Kodak, Rochester, NY).

Immunocytofluorescent Staining. ARBECs were seeded onto glass coverslips coated with type I rat tail collagen. After exposure to drugs for 24 h, cells were washed with PBS and fixed with PBS

containing 4% paraformaldehyde for 15 min and then permeabilized with 1% Triton X-100 for 20 min. After blocking with 4% dry skim milk in PBS buffer, cells were incubated with rabbit antibodies against ZO-1 (1:100) overnight at 4°C. After a brief wash, cells were then incubated with goat anti-rabbit FITC-conjugated secondary antibody (1:200; Leinco Technologies, Inc., St. Louis, MO) for 1 h. Finally, cells were washed again, mounted, and visualized by fluorescence microscopy (Carl Zeiss Inc., Thornwood, NY).

Transfection and Reporter Gene Assay. ARBECs were seeded onto 12-well plates coated with type I rat tail collagen. Cells were cotransfected with 0.4 μg of lac-Z vector and 0.8 μg of HRE-luciferase reporter gene, 1.5 kb of VEGF-luciferase reporter gene, or 1.2 kb of HRE-deleted VEGF-luciferase reporter gene, respectively (gifts from M.L. Kuo, National Taiwan University, Taipei, Taiwan). Plasmid DNA and Lipofectamine 2000 (10 μg/ml; Invitrogen) were premixed with Opti-MEM I (Invitrogen) separately for 5 min and then mix with each other for 25 min and then applied to the cells (500 μl/well). After 24-h transfection, the medium was replaced with fresh serum-free culture medium and exposed to drugs for 24 h for the detection of HRE luciferase and VEGF luciferase activity. To prepare lysates, 100 μl of reporter lysis buffer (Promega, Madison, WI) was added to each well, and cells were scraped from plates. The supernatant was collected after centrifugation at 15,000*g* for 3 min. Aliquots of cell lysates (20 μl) containing equal amounts of proteins were placed into wells of an opaque white 96-well microplate. The luciferase activity was determined using a dual-luciferase reporter assay system (Promega) and activity value was normalized to transfection efficiency monitored by the cotransfected lacZ vector.

Reverse Transcriptase-PCR and Quantitative Real Time-PCR. ARBECs were seeded onto six-well plates coated with type I rat tail collagen. After exposure to drugs for 6 or 24 h, total RNA were extracted using a TRIzol kit (MDBio, Inc., Taipei, Taiwan). Two micrograms of RNA were used for reverse transcription by using a commercial kit (Invitrogen, Carlsbad, CA). PCR was performed using an initial step of denaturation (5 min at 95°C), 30 cycles of amplification (95°C for 30 s, 60°C for 1 min, and 72°C for 30 s), and an extension (72°C for 2 min). PCR products were analyzed on 2% agarose gels. Quantitative real time-PCR was proceeded using SYBR Green I Master Mix and analyzed with a model 7900 Sequence Detector System (Applied Biosystems, Foster City, CA). After preincubation at 50°C for 2 min and 95°C for 10 min, the PCR was performed as 40 cycles of 95°C for 10 s and 60°C for 1 min. The threshold was set above the nontemplate control background and within the linear phase of target gene amplification to calculate the cycle number at which the transcript was detected (denoted as C_T). The oligonucleotide primers were: ZO-1: forward, 5′-GCGAGGCATCGTTCCTAATAAG-3′; reverse: 5′-TCGCCACCTGCTGTCTTTG-3′; VEGF: forward, 5′-ACGAAAGCGCAAGAAATCCC-3′; reverse, 5′-TTAACTCAAGCTGCCTCGCC-3′; and β-actin: forward, 5′-AGGCTCTTTTCCAGCCTTCCT-3′; reverse, 5′-GTCTTTACGGATGTCAACGTCACA-3′.

Enzyme-Linked Immunosorbent Assay. ARBECs were seeded onto 24-well plates coated with type I rat tail collagen. After exposure to drugs for 24 h, 100 μl of culture medium was collected and frozen at −80°C until measurement by Quantikine Rat VEGF Immunoassay ELISA kit (R&D Systems, Minneapolis, MN). After adding 50 μl of assay diluent into each microplate well, 50 μl of sample medium was then added and incubated for 2 h at room temperature on the shaker. After a brief wash, 100 μl of conjugate buffer was added and incubated for 1 h. Finally, 100 μl of substrate solution (hydrogen peroxide and chromogen tetramethylbenzidine) was added and incubated in the dark, and 100 μl of stop solution (diluted HCl) was added 30 min after. The absorbance was measured at 450 nm by an ELISA reader (Bio-Tek, Winooski, VT).

Increase of Blood-Brain Barrier Permeability by Ischemia-Reperfusion in Rat. Male Sprague-Dawley rats were obtained from the National Laboratory Animal Center of Taiwan and kept on a 12-h light/dark cycle with ad libitum access to food and water. Rats were acclimated to the environment for 7 days before the experiments. The rats (250~300 g) were then anesthetized with trichloroacetaldehyde (400 mg/kg), and two common carotid arteries were exposed and occluded by artery clips through a neck skin incision. Under an operating microscope, a piece of skull was removed through a head skin incision, and the middle cerebral artery was tied with a polyamide monofilament nonabsorbable suture (diameter, 150 μm; Johnson and Johnson) to produce ischemia, and rectal temperature was maintained at 37°C by external warming. Ninety minutes after occlusion, YC-1 (1 mg/kg) was injected into femoral vein just before untying of suture. Evans blue dye (100 mg/kg; Sigma) was injected into femoral vein 2 h after reperfusion. Rats were perfused with saline 4 h later through the left ventricle until colorless perfusion fluid was obtained from the right atrium. After decapitation, the brain was removed from the skull, and each hemicortex was dissected.

Samples were weighed and soaked in 1 ml of 50% trichloroacetic acid solution. After homogenization and centrifugation, the extracted Evans blue dye was diluted with ethanol (1:3), and fluorescence intensity was measured at excitation and emission wavelengths of 620 nm and 680 nm, respectively, using a fluorescence reader (Belayev et al., 1996). The tissue content of Evans blue dye was quantified from a linear standard curve derived from known amounts of the dye and was expressed as micrograms per microgram of tissue.

Immunohistochemistry. After ischemia/reperfusion, rats were anesthetized and perfused with saline and fixed with phosphate buffer containing 4% paraformaldehyde. After decapitation, the brain was removed from the skull, postfixed in 4% paraformaldehyde at 4°C overnight, and then stored in 30% sucrose solution at 4°C for 2 days. Frozen samples were cut into slices by a sliding microtome in 50-μm coronal sections. Brain slices were rinsed with PBS and then soaked in 3% H_2O_2 (Wako Pure Chemicals) solution for 15 min to block endogenous peroxidase activity. After blocking in 10% dry skim milk containing 0.5% Triton X-100 for 1 h, slices were incubated with mouse antibodies against HIF-1α (1:100; Chemicon International, Temecula, CA) overnight at 4°C. After a brief wash, slices were then incubated with horse anti-mouse biotinylated secondary antibodies, and processed with avidin-biotin complex system (Vector Laboratories, Burlingame, CA), which was visualized by incubating with 0.5 mg/ml diaminobenzidine-HCl (Sigma) and 0.01% H_2O_2 in PBS. The diaminobenzidine-HCl reaction was stopped by rinsing slices with PBS.

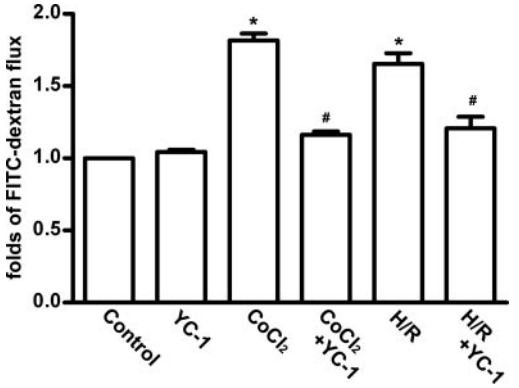

Fig. 1. Inhibition by YC-1 on $CoCl_2$- or H/R-induced increase of paracellular permeability in ARBECs. ARBECs cultured in cell culture inserts were pretreated with YC-1 (10 μM) for 30 min and then either treated with $CoCl_2$ (100 μM) for another 24 h or exposed to 24-h hypoxia followed by 4-h reoxygenation (H/R). Leakage of FITC-dextran was collected in the lower compartment. The data represent the mean ± S.E.M. from four independent experiments. *, $p < 0.05$, compared with control group. #, $p < 0.05$, compared with $CoCl_2$-treated group or H/R group.

Statistics. Values are expressed as mean ± S.E.M. of at least three experiments. Results were analyzed with one-way analysis of variance, followed by Neuman-Keuls. Significance was defined as $p < 0.05$.

Results

Inhibition by YC-1 on Increase of Paracellular Permeability and Destruction of ZO-1 in Response to Either $CoCl_2$ or Hypoxia/Reoxygenation Treatment in ARBECs. Exposure of ARBECs to chemical hypoxia-inducing agent $CoCl_2$ (100 μM) resulted in a significant increase (1.82-fold) of paracellular permeability within 24 h compared with control, and this effect was quantified by measuring FITC-dextran flux through paracellular monolayers in culture insert system after 24-h treatment (Fig. 1). We found that pretreatment with YC-1 (10 μM) for 30 min inhibited $CoCl_2$-induced increase of paracellular permeability, whereas YC-1 alone did not affect the paracellular flux of FITC-dextran. Total amounts of FITC-dextran collected in the lower compartment of culture insert system after 24 h revealed that YC-1 inhibited $CoCl_2$-induced increase of permeability by 80.0 ± 4.8% ($n = 4$). In addition, 24-h hypoxia followed by 4-h reoxygenation (H/R) also significantly increased paracellular permeability, and YC-1 (10 μM) pretreatment antagonized H/R-induced increase of paracellular permeability by 68.4 ± 8.0% ($n = 4$). To confirm that the increase of permeability was not due to cytotoxicity, cell viability was assessed by MTT. There was no significant difference in viability after drug treatment.

To determine whether $CoCl_2$- and H/R-induced increase of paracellular permeability was due to alteration in the expres-

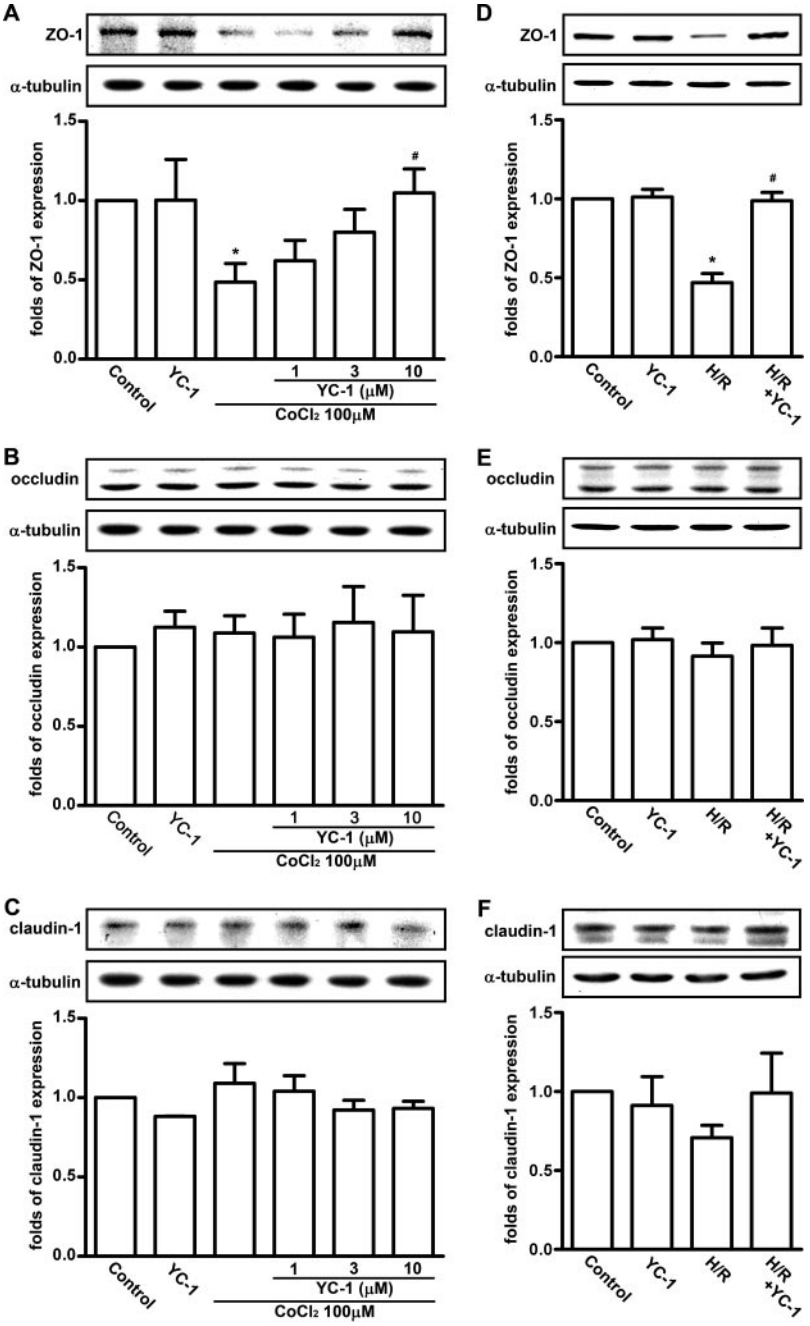

Fig. 2. Antagonism by YC-1 on the reduction of ZO-1 proteins in response to $CoCl_2$ or H/R treatments. ARBECs pretreated with different concentrations of YC-1 were then either exposed to $CoCl_2$ (100 μM) for another 24 h (A–C) or suffered from 24-h hypoxia followed by 4-h reoxygenation (D–F). Cell lysates were prepared and followed by electrophoresis and immunoblotting for the determination of protein levels of ZO-1 (A and D), occludin (B and E), and claudin-1 (C and F). The data represent the mean ± S.E.M. from at least three independent experiments. *, $p < 0.05$, compared with control group. #, $p < 0.05$, compared with $CoCl_2$- or H/R-treated group.

sion of TJ proteins, ZO-1, occludin, and claudin-1 expression levels were examined by Western blotting. As shown in Fig. 2A, treatment with $CoCl_2$ reduced ZO-1 protein expression levels by 51.4 ± 11.8% (n = 4), and pretreatment of YC-1 antagonized $CoCl_2$-induced reduction of ZO-1 expression in a concentration-dependent manner. Furthermore, as shown in Fig. 2D, ZO-1 protein expression levels after H/R were reduced by 53.1 ± 5.8%, and pretreatment of 10 μM YC-1 also antagonized H/R-induced reduction of ZO-1 expression. However, $CoCl_2$, H/R, or YC-1 treatment exerted no significant effect on occludin and claudin-1 (Fig. 2, B, C, E, and F).

To examine the structural basis for the alteration in permeability, the distribution of ZO-1 was visualized by immunofluorescent staining. The result also revealed that the arrangement of ZO-1 was disorganized in response to $CoCl_2$ or H/R treatment, and YC-1 antagonized the destruction of ZO-1 (Fig. 3). These results were consistent with the inhibitory effect of YC-1 on FITC-dextran permeability as shown in Fig. 1, indicating that YC-1 is capable of inhibiting $CoCl_2$- and H/R-induced ZO-1 destruction and increase of paracellular permeability.

Inhibition by YC-1 on $CoCl_2$-Induced Increase of Paracellular Permeability in ARBECs Is Not through cGMP and PKG Pathway. Because YC-1 has been characterized as a nitric oxide (NO) sensitizer and regulates intracellular cGMP concentration through the enhancement of sensitivity of soluble guanylate cyclase to NO (Chien et al., 2005), we then examined whether the inhibitory effect of YC-1 was through NO-cGMP-PKG pathway. It was found that L-NAME (nonselective NOS inhibitor; 0.5 mM) attenuated the protective effect of YC-1 in response to $CoCl_2$ treatment. However, cotreatment with 20 μM ODQ (sGC inhibitor) or 1 μM KT5823 (PKG inhibitor) did not antagonize the protective effect of YC-1 against $CoCl_2$-induced hyperpermeability (Fig. 4A). In addition, treatment of 30 μM 8-Br-cGMP also did not exert the similar effect as YC-1 to inhibit ZO-1 destruction after $CoCl_2$ treatment (Fig. 4B). These results suggest that cGMP and PKG is not involved in the protective action of YC-1.

Inhibition by YC-1 on $CoCl_2$-Induced HIF-1α Accumulation and VEGF Production in ARBECs. It is well known that $CoCl_2$ exposure results in the up-regulation of HIF-1α and downstream target gene expression in many cell types (Gleadle et al., 1995; Ke et al., 2005). We then investigated the effect of YC-1 on HIF-1α accumulation in ARBECs. ARBECs were pretreated with different concentrations of YC-1 for 30 min and then exposed to $CoCl_2$ (100 μM) for another 6 h. As shown in Fig. 5A, Western blotting demonstrated that $CoCl_2$-induced HIF-1α accumulation was inhibited by YC-1 in a concentration-dependent manner. In addition, we also examined $CoCl_2$-induced enhancement of HIF-1 activity by using HRE-luciferase reporter gene. ARBECs were transfected with reporter gene and were then exposed to $CoCl_2$ in the absence or presence of YC-1 for another 24 h. Cell lysates were prepared, and the luciferase activities were analyzed. As shown in Fig. 5B, $CoCl_2$-induced increase of HRE-luciferase activity was also concentration-dependently inhibited by YC-1.

Because VEGF is one of the well known downstream target gene of HIF-1 related to vascular biology (Forsythe et al., 1996; Sharp and Bernaudin, 2004), we then investigated whether VEGF is involved in the protective effect of YC-1

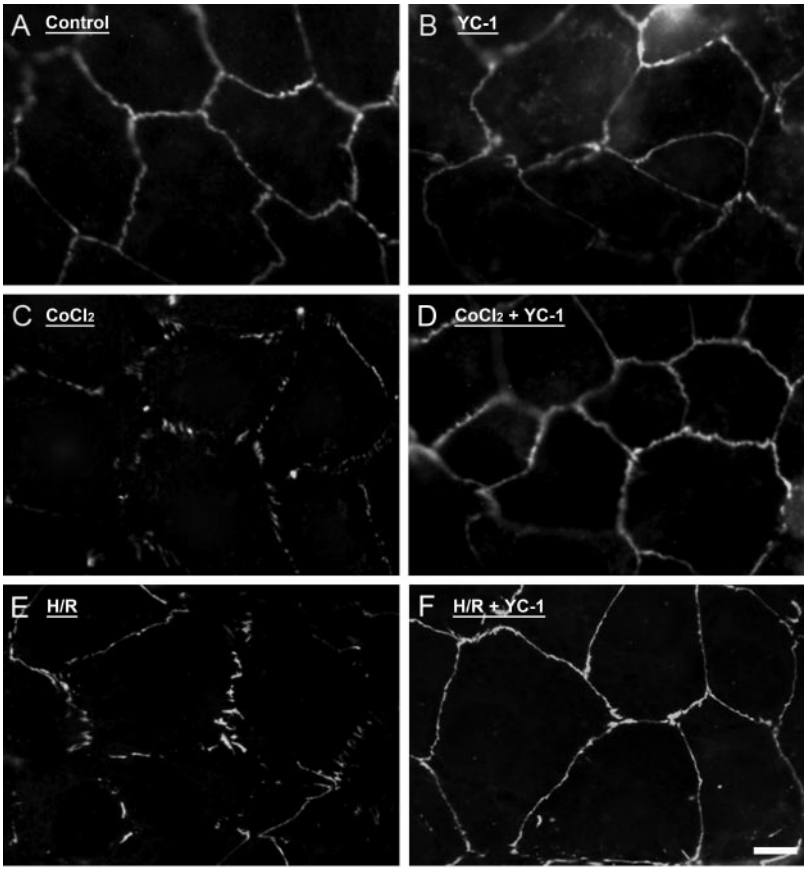

Fig. 3. Effect of YC-1 on the destruction of ZO-1 in response to $CoCl_2$ or H/R treatments. ARBECs grown on coverslips were pretreated with YC-1 (10 μM) for 30 min and then either exposed to $CoCl_2$ (100 μM) for another 24 h or 24-h hypoxia followed by 4-h reoxygenation. Immunofluorescence of ZO-1 in control (A), YC-1 alone (B), $CoCl_2$ treatment (C), $CoCl_2$ plus YC-1 (D), H/R treatment (E), and H/R puls YC-1 (F). Scale bar, 5 μm.

against $CoCl_2$-induced increase of paracellular permeability in ARBECs. First of all, we demonstrated that $CoCl_2$ treatment increased VEGF-luciferase activity when cells were transfected with full-length of VEGF-luciferase reporter gene (1.5 kb) but not with HRE-deleted VEGF-luciferase reporter gene (1.2 kb; Fig. 6A). This result confirmed that the stimulating effect of $CoCl_2$ on VEGF expression is through HIF-1 binding to HRE promoter region of VEGF gene (Liu et al., 1995; Ema et al., 1997). Furthermore, it was found that 1.5-kbVEGF-luciferase activity enhanced by $CoCl_2$ treatment was antagonized by YC-1 in a concentration-dependent manner (Fig. 6B). Pretreatment of YC-1 (10 μM) also inhibited $CoCl_2$-induced VEGF mRNA expression by using quantitative real-time PCR measurement (Fig. 6C). Furthermore, VEGF protein content in cultured medium measured by ELISA kit revealed that there was a significant increase (4.0-fold) after 24-h exposure of $CoCl_2$ compared with control (160.7 ± 25.4 pg/10^5 cells and 40.1 ± 0.7 pg/10^5 cells, respectively), which was abolished by YC-1 treatment (46.1 ± 6.2 pg/10^5 cells; Fig. 6D). These results indicate that HIF-1α accumulation and VEGF production in response to chemical hypoxia is inhibited by YC-1 in ARBECs.

Involvement of VEGF in the Increase of Paracellular Permeability and Destruction of ZO-1 after Either $CoCl_2$ or H/R Treatment in ARBECs. It has been reported that BBB permeability is increased by VEGF (Schoch et al., 2002), we then examined whether VEGF production affects ZO-1 expression. We evaluated the expression levels of protein as well as mRNA. It was found that VEGF (20 ng/ml), $CoCl_2$, or H/R treatment reduced ZO-1 protein expression; however, VEGF antibody administration antagonized the ZO-1 reduction caused by $CoCl_2$ exposure or H/R treatment (Fig. 7, A and B), whereas IgG administration served as negative control. In addition, treatment of VEGF for 6 h or treatment with $CoCl_2$ for 24 h reduced ZO-1 mRNA expres-

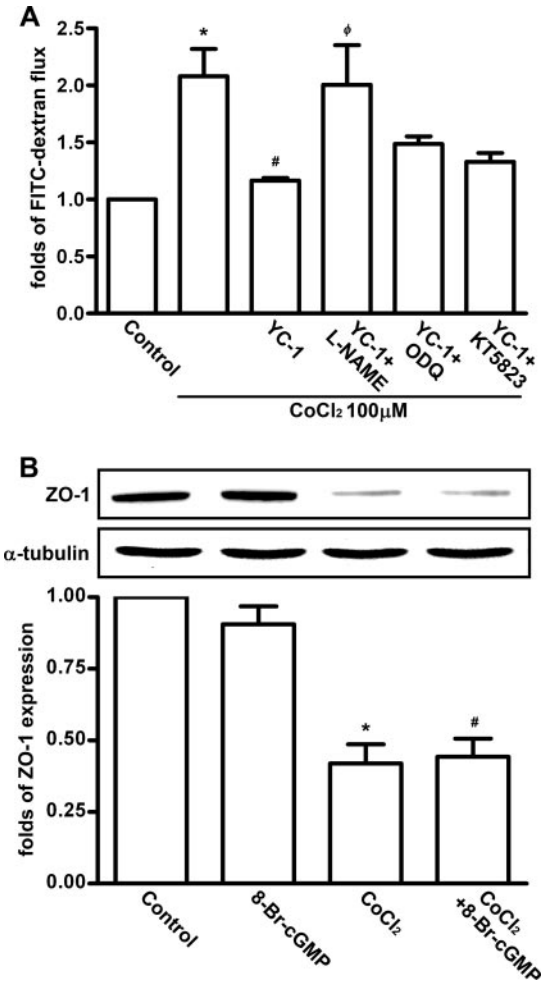

Fig. 4. Inhibition by YC-1 on $CoCl_2$-induced increase of paracellular permeability in ARBECs is not through cGMP and PKG. A, ARBECs were cultured in cell culture inserts and pretreated with YC-1 (10 μM) for 30 min and then exposed to $CoCl_2$ (100 μM). Leakage of FITC-dextran was collected in the lower compartment after 24-h treatment of $CoCl_2$. B, ARBECs were pretreated with 8-Br-cGMP (30 μM) for 30 min and then exposed to $CoCl_2$ (100 μM) for another 24 h. Cell lysates were prepared and followed by electrophoresis and immunoblotting for the determination of protein levels of ZO-1. Note that L-NAME but not ODQ or KT5823 attenuates the protective effect of YC-1 in response to $CoCl_2$-induced injury. Treatment of 8-Br-cGMP did not exert the similar protective effect as YC-1. The data represent the mean ± S.E.M. from at least three independent experiments. *, $p < 0.05$, compared with control group. #, $p < 0.05$, compared with $CoCl_2$-treated group. ϕ, $p < 0.05$, compared with $CoCl_2$ + YC-1 group.

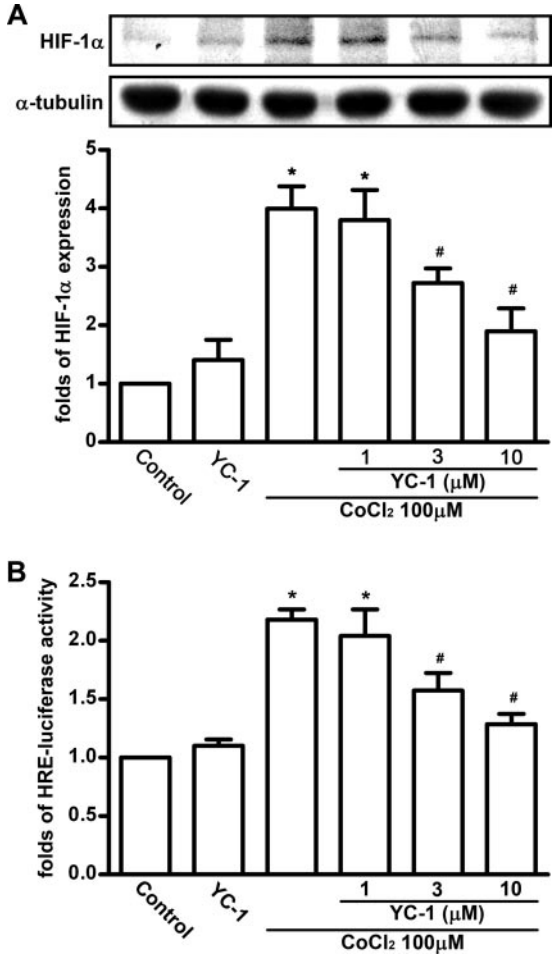

Fig. 5. Inhibition by YC-1 on $CoCl_2$-induced HIF-1α accumulation in endothelial cells. A, ARBECs were pretreated with different concentrations of YC-1 for 30 min and then exposed to $CoCl_2$ (100 μM) for another 24 h. Cell lysates were prepared and followed by electrophoresis and immunoblotting for the determination of protein levels of HIF-1α. B, cells cotransfected with HRE-luciferase reporter gene and lac-Z vector were exposed to $CoCl_2$ with or without different concentrations of YC-1. The data represent the mean ± S.E.M. from at least three independent experiments. *, $p < 0.05$, compared with control group. #, $p < 0.05$, compared with $CoCl_2$-treated group.

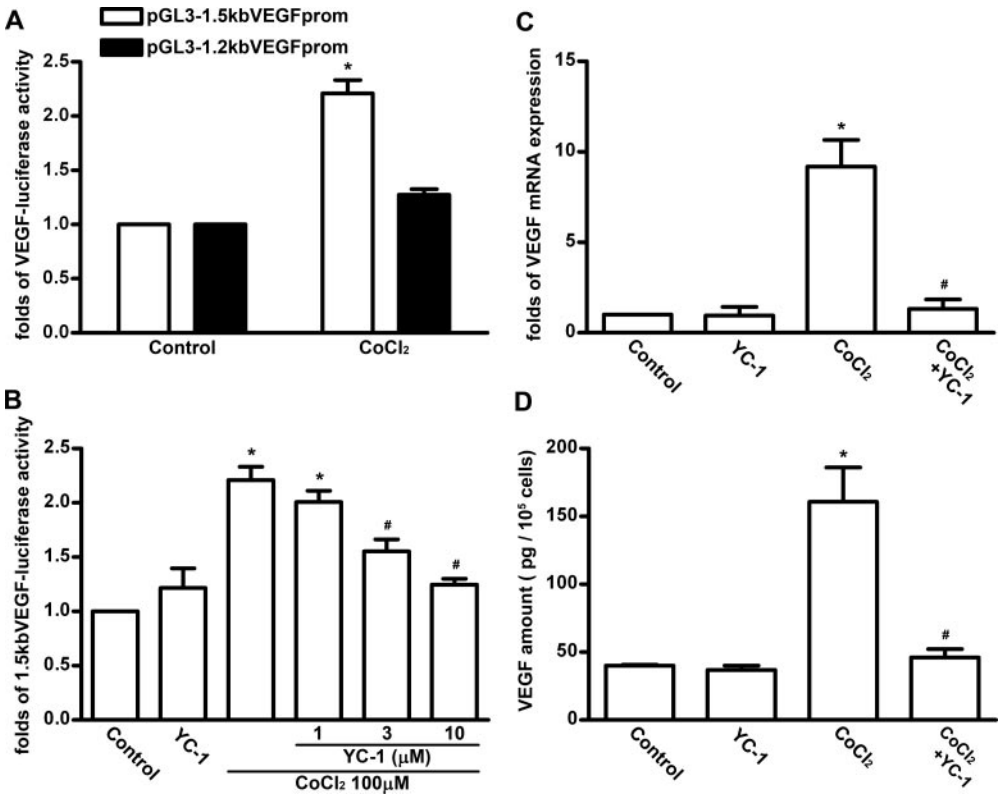

Fig. 6. Inhibition by YC-1 on $CoCl_2$-induced VEGF production in endothelial cells. A, increase of VEGF-luciferase activity by $CoCl_2$ (100 μM) was observed by transfection with full-length of VEGF-luciferase reporter gene (1.5 kb) but not with HRE-deleted VEGF-luciferase reporter gene (1.2 kb). B, cells cotransfected with 1.5 or 1.2 kb of VEGF-luciferase reporter gene and lac-Z vector were exposed to $CoCl_2$ in the presence or absence of YC-1. Note that YC-1 antagonized the increase of VEGF reporter gene activity and VEGF mRNA expression induced by $CoCl_2$ (C). D, culture medium was collected for the measurement of VEGF using an ELISA kit after treatment with YC-1 (10 μM) plus $CoCl_2$ (100 μM) for 24 h. The data represent the mean ± S.E.M. from at least three independent experiments. *, $p < 0.05$, compared with control group. #, $p < 0.05$, compared with $CoCl_2$-treated group.

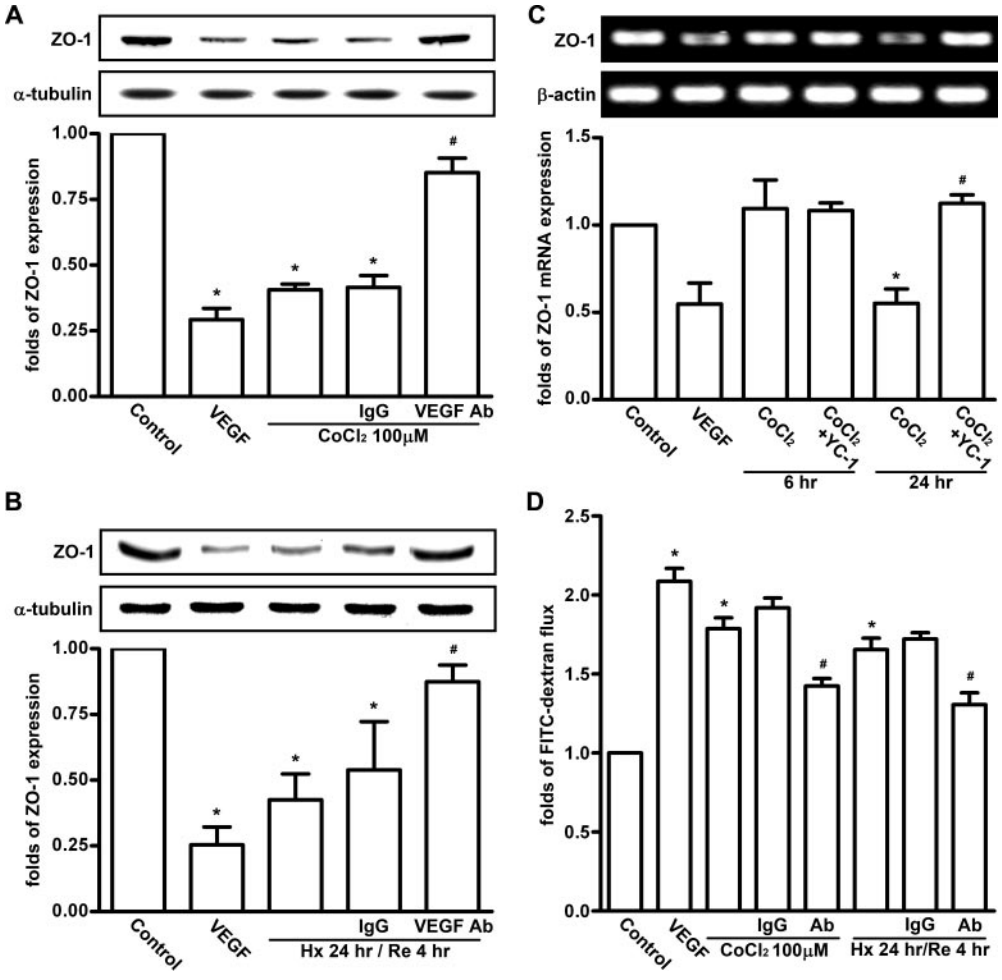

Fig. 7. Involvement of VEGF in $CoCl_2$- or H/R-induced increase of paracellular permeability. ARBECs were either exposed to $CoCl_2$ (100 μM) (A) or suffered from H/R in the presence or absence of VEGF antibody (Ab, 1 μg/ml) (B) for indicated time intervals. IgG antibody (IgG, 1 μg/ml) or VEGF (20 ng/ml) treatment was used as negative and positive control, respectively. Cell lysates were prepared after treatment and protein levels of ZO-1 were determined. C, cell lysates were prepared after 6- or 24-h treatment of $CoCl_2$ and followed by reverse transcriptase-polymerase chain reaction for the determination of mRNA levels of ZO-1. Note that $CoCl_2$-induced increase of VEGF is involved in permeability increase, which is antagonized by concomitant treatment with YC-1. D, in cell culture insert systems, leakage of FITC-dextran was collected in the lower compartment after 24-h $CoCl_2$ treatment or 24-h hypoxia followed by 4-h reoxygenation. The data represent the mean ± S.E.M. from at least three independent experiments. *, $p < 0.05$, compared with control group. #, $p < 0.05$, compared with $CoCl_2$- or H/R-treated group.

sion by 45.2 ± 12.0% and 44.9 ± 8.3%, respectively. The reduction in ZO-1 mRNA expression in response to $CoCl_2$ was abolished by concomitant treatment with YC-1 (Fig. 7C). We further examined the effect of VEGF antibody on the permeability potentiating action of $CoCl_2$ or H/R treatment. As shown in Fig. 7D, VEGF (20 ng/ml) used as positive control was found to increase FITC-dextran flux through paracellular monolayers by 2.1-fold. Exposure of ARBECs to either $CoCl_2$ or H/R increased the paracellular permeability by 1.8- and 1.7-fold, respectively, and VEGF antibody-inhibited $CoCl_2$ or H/R induced an increase of paracellular permeability by 46.0 ± 6.9% and 53.2 ± 7.5% ($n = 4$), respectively. This result indicates that $CoCl_2$ or H/R caused an increase of paracellular permeability, which may result from the enhancement of VEGF production.

To further examine the structural basis for the alteration in permeability, the distribution of ZO-1 was visualized by immunofluorescent staining. The result reveals that VEGF antibody antagonized the destruction of ZO-1 in response to $CoCl_2$ or H/R treatment (Fig. 8), which is consistent with the effect of antibody on permeability increase. These results indicate that VEGF is involved in $CoCl_2$- or H/R-induced increase of paracellular permeability and destruction of ZO-1 in ARBECs.

Inhibition by YC-1 on Ischemia/Reperfusion-Induced Increase of BBB Permeability and HIF-1α Accumulation in Rats. The results mentioned above show that YC-1 exerts protection of ARBECs against $CoCl_2$- or H/R-induced increase of paracellular permeability in vitro; we then investigated whether YC-1 exerts this protective effect in vivo. Rats were ligated in bilateral common carotid arteries and one middle cerebral artery for 1.5 h and reperfused for 6 h. Evans blue dye was used to serve as a marker of albumin extravasation. As shown in Fig. 9A, the ipsilateral side but not the contralateral side exhibited a marked increase (9.5-fold) of permeability (20.35 ± 3.62 μg/g of tissue and 2.15 ± 0.97 μg/g of tissue, respectively) (Belayev et al., 1996). Treatment of YC-1 strongly reduced the increase of permeability by 76.8% (5.35 ± 1.52 μg/g tissue; Fig. 9B). Furthermore, immunostaining demonstrated that ischemia/reperfusion increased HIF-1α accumulation in both cerebral blood vessels (arrowhead) and nonvascular cells (Fig. 9C, middle), and administration of YC-1 inhibited the accumulation of HIF-1α (Fig. 9C, lower). These results indicate that YC-1 is able to protect BBB from hyperpermeability induced by ischemia/reperfusion in animal model.

Discussion

Tight junction barrier in endothelial cells of cerebral microvasculature serves as a frontline defense, protecting neurons and glia cells from harmful insults. Under pathological conditions, tight junction proteins may undergo rearrangement or alteration in protein expression (Wang et al., 2001; Mark and Davis, 2002). Hypoxia is an important pathogenic factor for the alteration of tight junction proteins and induction of vascular leakage in the brain. It has been reported that the dominant negative form of HIF-1α inhibits the hypoxia-induced activity of VEGF promoter in Hep3B cells (Forsythe et al., 1996), and exposure to hypoxia leads to a significant increase of VEGF mRNA and protein in mouse brain, which is correlated with the severity of the hypoxia (Schoch et al., 2002). Hypoxia-induced hyperpermeability of brain microvascular endothelial cell monolayers is mediated by VEGF in an autocrine manner (Fischer et al., 1999). In this study, we found that hypoxia caused an increase of BBB endothelial permeability and a destruction of ZO-1 partially by acting through HIF-1α-induced VEGF production. However, other tight junction proteins, such as occludin and claudin-1, are not affected. We also found that VEGF inhibits ZO-1 mRNA expression, indicating that VEGF regulates ZO-1 expression at the transcription level. This result is consistent with that reported by Ghassemifar et al. (2006); i.e., VEGF has a dual capability with respect to the regulation of the expression of some TJ proteins at the transcriptional and post-translational levels on different cell types. However, the exact mechanisms regarding the regulation on VEGF production and VEGF-mediated expression of TJ proteins by HIF-1α still require further investigation. Here, we demonstrated that YC-1 was able to abolish these harmful effects in response to hypoxia

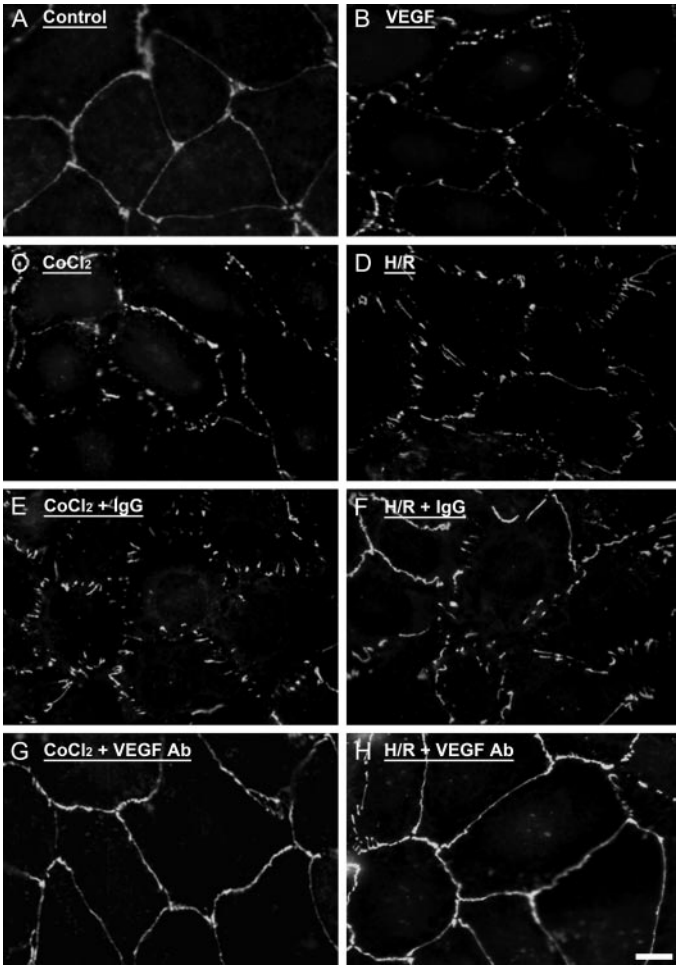

Fig. 8. Involvement of VEGF in the destruction of ZO-1 arrangement in response to $CoCl_2$ or H/R treatment. ARBECs grown on coverslips were either treated with $CoCl_2$ (100 μM) for 24 h or exposed to 24-h hypoxia followed by 4-h reoxygenation in the absence (C and D) or presence (G and H) of VEGF antibody (1 μg/ml). IgG antibody (1 μg/ml) was used as negative control (E and F). Note that compared with control (A), treatment with either $CoCl_2$ or H/R caused the destruction of ZO-1 (C and D), which was inhibited by coadministration of VEGF antibody (G and H). VEGF (20 ng/ml) treatment alone was used as positive control (B). Scale bar, 5 μm.

through inhibition of HIF-1α accumulation and VEGF production. Other factors, except VEGF, may also contribute to hypoxia-induced hyperpermeability, because YC-1 is much more effective than VEGF antibody in the inhibition of permeability.

In addition to the protective action of YC-1 in cell cultures, in vivo study also reveals that YC-1 is able to inhibit ischemia/reperfusion-induced increase of BBB permeability in rats. Nevertheless, the responses in animal study may be more complicated, and focus on a single intracellular pathway or cell type might not be sufficient. The neurovascular unit is composed of endothelial cells, astrocytes, pericytes, adjacent neurons, extracellular matrix, and basal lamina (Hawkins and Davis, 2005). After ischemia/reperfusion, perturbations in neurovascular functional integrity initiate several cascades of injury. Upstream signals such as oxidative stress, together with neutrophil and/or platelet interactions with activated endothelium, up-regulate matrix metalloproteinases, plasminogen activators, other proteases, and inflammatory cytokines, which degrade matrix and lead to the increase of BBB permeability (Lo et al., 2003; Hawkins and Davis, 2005). Thus, the origin of protective effects of YC-1 other than endothelial cells in animal studies cannot be excluded. Using VEGF inhibitor or neutralizing antibody may also be useful to certify the protective effect in ischemia/reperfusion rats.

YC-1 is not only a suppressor of HIF-1α accumulation (Kim et al., 2006) but also a NO sensitizer. YC-1 regulates intracellular cGMP concentration through the enhancement of sensitivity of soluble guanylate cyclase to NO (Ko et al., 1994). On the one hand, NO has emerged as an important regulator in controlling vascular tone (Shesely et al., 1996). However, there are controversies regarding its role in the modulation of microvascular permeability. There is some evidence to support the idea that activation of nitric-oxide synthase and NO production results in an increase of microvascular permeability in response to hypoxia (Mark et al., 2004) or inflammatory mediators (Bove et al., 2001), whereas other reports demonstrate that NO is a permeability-decreasing factor and maintain junctional integrity (Kurose et al., 1994; Predescu et al., 2005). Furthermore, there are also disputes about the role of cGMP/PKG in vascular permeability. Some evidence supports the idea that cGMP has a barrier-enhancing effect (Moldobaeva et al., 2006) and protects microvessels from injury induced by reactive oxygen species (Pearse et al., 2003), whereas others considered cGMP a permeability-increasing factor under both normoxic and hypoxic conditions (Fischer et al., 1999). Our results show that L-NAME (a nitric-oxide synthase inhibitor) attenuated the protective effect of YC-1 in response to $CoCl_2$-induced injury. However, cotreatment with ODQ or KT5823 (sGC inhibitor and PKG inhibitor, respectively) did not affect the protective effect of YC-1, and treatment of 8-Br-cGMP did not exert protection similar to that of YC-1. These results indicate that NO but not cGMP or PKG is an additional protective effector to reduce $CoCl_2$-induced BBB permeability.

In addition to VEGF, other factors may also contribute to barrier dysfunction, such as TGF-β. TGF-β can be up-regulated under hypoxia through HIF-1α and increases endothelial permeability through the reorganization of adherence junctions and focal adhesion complexes (Lu et al., 2006). Furthermore, evidence indicates that there is cross-talk between growth factors, and cell signaling might escape from one pathway to aggravate another compensatory pathway. Expression of VEGF and VEGF receptor were increased by TGF-β and matrix metalloproteinase expression, which can be activated by hypoxia (Jeon et al., 2007). Because HIF-1α is a transcription factor acting upstream of many factors regulating hypoxic response in many cell types, we therefore believe that HIF-1α inhibitor may have more therapeutic benefit in preventing BBB destruction and brain edema in patients suffering from stroke compared with either VEGF inhibitor alone or agents targeting tight junctions.

In summary, the results from this study clearly demonstrate that ARBECs undergo molecular and functional changes under hypoxia, and these phenomena can be abolished by the treatment of YC-1. Furthermore, YC-1 protects the BBB from ischemia/reperfusion-induced hyperpermeability in an animal model and inhibits HIF-1α accumulation in cerebral blood vessels and nonvascular cells. Therefore, YC-1 may have the potential to be developed as a novel drug to inhibit the increase of BBB permeability after ischemia.

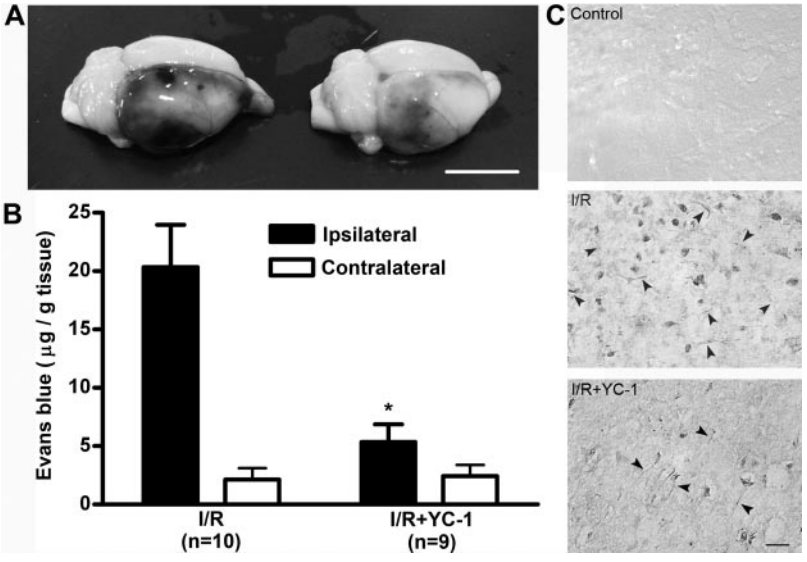

Fig. 9. Inhibition by YC-1 on ischemia/reperfusion-induced increase of BBB permeability and HIF-1α accumulation in rats. A, right middle cerebral artery and two common carotid arteries were transiently ligated for 1.5 h and YC-1 (1 mg/kg) was injected from femoral vein just before reperfusion. Evans blue dye (100 mg/kg) was injected into femoral vein 2 h after reperfusion, and permeability was evaluated 4 h later. Scale bar, 1 cm. B, Evans blue dye was extracted from each hemicortex as a marker of albumin extravasation. C, immunostaining of HIF-1α shows that ischemia/reperfusion (I/R) increased the immunostaining of HIF-1α in cerebral blood vessels (arrowhead) and nonvascular cells (middle). Administration of YC-1 inhibited the accumulation of HIF-1α (bottom). Scale bar, 50 μm. The data represent the mean ± S.E.M. (n ≥9). *, $p < 0.05$, compared with I/R group.

Acknowledgments

We thank the National Research Council of Canada for providing us the cell line ARBECs.

References

Andriopoulou P, Navarro P, Zanetti A, Lampugnani MG, and Dejana E (1999) Histamine induces tyrosine phosphorylation of endothelial cell-to-cell adherens junctions. *Arterioscler Thromb Vasc Biol* **19:**2286–2297.

Belayev L, Busto R, Zhao W, and Ginsberg MD (1996) Quantitative evaluation of blood-brain barrier permeability following middle cerebral artery occlusion in rats. *Brain Res* **739:**88–96.

Bove K, Neumann P, Gertzberg N, and Johnson A (2001) Role of ecNOS-derived NO in mediating TNF-induced endothelial barrier dysfunction. *Am J Physiol Lung Cell Mol Physiol* **280:**L914–L922.

Chien WL, Liang KC, Teng CM, Kuo SC, Lee FY, and Fu WM (2005) Enhancement of learning behaviour by a potent nitric oxide-guanylate cyclase activator YC-1. *Eur J Neurosci* **21:**1679–1688.

Connolly DT (1991) Vascular permeability factor: a unique regulator of blood vessel function. *J Cell Biochem* **47:**219–223.

Dejana E (2004) Endothelial cell-cell junctions: happy together. *Nat Rev Mol Cell Biol* **5:**261–270.

Dvorak HF, Brown LF, Detmar M, and Dvorak AM (1995) Vascular permeability factor/vascular endothelial growth factor, microvascular hyperpermeability, and angiogenesis. *Am J Pathol* **146:**1029–1039.

Ema M, Taya S, Yokotani N, Sogawa K, Matsuda Y, and Fujii-Kuriyama Y (1997) A novel bHLH-PAS factor with close sequence similarity to hypoxia-inducible factor 1alpha regulates the VEGF expression and is potentially involved in lung and vascular development. *Proc Natl Acad Sci U S A* **94:**4273–4278.

Feldman GJ, Mullin JM, and Ryan MP (2005) Occludin: structure, function and regulation. *Adv Drug Deliv Rev* **57:**883–917.

Fischer S, Clauss M, Wiesnet M, Renz D, Schaper W, and Karliczek GF (1999) Hypoxia induces permeability in brain microvessel endothelial cells via VEGF and NO. *Am J Physiol* **276:**C812–C820.

Forsythe JA, Jiang BH, Iyer NV, Agani F, Leung SW, Koos RD, and Semenza GL (1996) Activation of vascular endothelial growth factor gene transcription by hypoxia-inducible factor 1. *Mol Cell Biol* **16:**4604–4613.

Garberg P, Ball M, Borg N, Cecchelli R, Fenart L, Hurst RD, Lindmark T, Mabondzo A, Nilsson JE, Raub TJ, et al. (2005) In vitro models for the blood-brain barrier. *Toxicol In Vitro* **19:**299–334.

Ghassemifar R, Lai CM, and Rakoczy PE (2006) VEGF differentially regulates transcription and translation of ZO-1alpha+ and ZO-1alpha- and mediates trans-epithelial resistance in cultured endothelial and epithelial cells. *Cell Tissue Res* **323:**117–125.

Gleadle JM, Ebert BL, Firth JD, and Ratcliffe PJ (1995) Regulation of angiogenic growth factor expression by hypoxia, transition metals, and chelating agents. *Am J Physiol* **268:**C1362–C1368.

Gloor SM, Wachtel M, Bolliger MF, Ishihara H, Landmann R, and Frei K (2001) Molecular and cellular permeability control at the blood-brain barrier. *Brain Res Brain Res Rev* **36:**258–264.

González-Mariscal L, Betanzos A, and Avila-Flores A (2000) MAGUK proteins: structure and role in the tight junction. *Semin Cell Dev Biol* **11:**315–324.

Hawkins BT and Davis TP (2005) The blood-brain barrier/neurovascular unit in health and disease. *Pharmacol Rev* **57:**173–185.

Hsu HK, Juan SH, Ho PY, Liang YC, Lin CH, Teng CM, and Lee WS (2003) YC-1 inhibits proliferation of human vascular endothelial cells through a cyclic GMP-independent pathway. *Biochem Pharmacol* **66:**263–271.

Jeon SH, Chae BC, Kim HA, Seo GY, Seo DW, Chun GT, Kim NS, Yie SW, Byeon WH, Eom SH, et al. (2007) Mechanisms underlying TGF-beta1-induced expression of VEGF and Flk-1 in mouse macrophages and their implications for angiogenesis. *J Leukoc Biol* **81:**557–566.

Ke Q, Kluz T, and Costa M (2005) Down-regulation of the expression of the FIH-1 and ARD-1 genes at the transcriptional level by nickel and cobalt in the human lung adenocarcinoma A549 cell line. *Int J Environ Res Public Health* **2:**10–13.

Kim HL, Yeo EJ, Chun YS, and Park JW (2006) A domain responsible for HIF-1alpha degradation by YC-1, a novel anticancer agent. *Int J Oncol* **29:**255–260.

Ko FN, Wu CC, Kuo SC, Lee FY, and Teng CM (1994) YC-1, a novel activator of platelet guanylate cyclase. *Blood* **84:**4226–4233.

Kurose I, Wolf R, Grisham MB, and Granger DN (1994) Modulation of ischemia/reperfusion-induced microvascular dysfunction by nitric oxide. *Circ Res* **74:**376–382.

Liu Y, Cox SR, Morita T, and Kourembanas S (1995) Hypoxia regulates vascular endothelial growth factor gene expression in endothelial cells. Identification of a 5′ enhancer. *Circ Res* **77:**638–643.

Lo EH, Dalkara T, and Moskowitz MA (2003) Mechanisms, challenges and opportunities in stroke. *Nat Rev Neurosci* **4:**399–415.

Lu Q, Harrington EO, Jackson H, Morin N, Shannon C, and Rounds S (2006) Transforming growth factor-beta1-induced endothelial barrier dysfunction involves Smad2-dependent p38 activation and subsequent RhoA activation. *J Appl Physiol* **101:**375–384.

Mark KS, Burroughs AR, Brown RC, Huber JD, and Davis TP (2004) Nitric oxide mediates hypoxia-induced changes in paracellular permeability of cerebral microvasculature. *Am J Physiol Heart Circ Physiol* **286:**H174–H180.

Mark KS and Davis TP (2002) Cerebral microvascular changes in permeability and tight junctions induced by hypoxia-reoxygenation. *Am J Physiol Heart Circ Physiol* **282:**H1485–H1494.

Moldobaeva A, Welsh-Servinsky LE, Shimoda LA, Stephens RS, Verin AD, Tuder RM, and Pearse DB (2006) Role of protein kinase G in barrier-protective effects of cGMP in human pulmonary artery endothelial cells. *Am J Physiol Lung Cell Mol Physiol* **290:**L919–L930.

Pearse DB, Shimoda LA, Verin AD, Bogatcheva N, Moon C, Ronnett GV, Welsh LE, and Becker PM (2003) Effect of cGMP on lung microvascular endothelial barrier dysfunction following hydrogen peroxide. *Endothelium* **10:**309–317.

Predescu D, Predescu S, Shimizu J, Miyawaki-Shimizu K, and Malik AB (2005) Constitutive eNOS-derived nitric oxide is a determinant of endothelial junctional integrity. *Am J Physiol Lung Cell Mol Physiol* **289:**L371–L381.

Salceda S and Caro J (1997) Hypoxia-inducible factor 1α (HIF-1α) protein is rapidly degraded by the ubiquitin-proteasome system under normoxic conditions. Its stabilization by hypoxia depends on redox-induced changes. *J Biol Chem* **272:**22642–22647.

Schoch HJ, Fischer S, and Marti HH (2002) Hypoxia-induced vascular endothelial growth factor expression causes vascular leakage in the brain. *Brain* **125:**2549–2557.

Senger DR, Galli SJ, Dvorak AM, Perruzzi CA, Harvey VS, and Dvorak HF (1983) Tumor cells secrete a vascular permeability factor that promotes accumulation of ascites fluid. *Science* **219:**983–985.

Sharp FR and Bernaudin M (2004) HIF1 and oxygen sensing in the brain. *Nat Rev Neurosci* **5:**437–448.

Shesely EG, Maeda N, Kim HS, Desai KM, Krege JH, Laubach VE, Sherman PA, Sessa WC, and Smithies O (1996) Elevated blood pressures in mice lacking endothelial nitric oxide synthase. *Proc Natl Acad Sci U S A* **93:**13176–13181.

Wang GL, Jiang BH, Rue EA, and Semenza GL (1995) Hypoxia-inducible factor 1 is a basic-helix-loop-helix-PAS heterodimer regulated by cellular O2 tension. *Proc Natl Acad Sci U S A* **92:**5510–5514.

Wang W, Dentler WL, and Borchardt RT (2001) VEGF increases BMEC monolayer permeability by affecting occludin expression and tight junction assembly. *Am J Physiol Heart Circ Physiol* **280:**H434–H440.

Yeo EJ, Chun YS, Cho YS, Kim J, Lee JC, Kim MS, and Park JW (2003) YC-**1:** a potential anticancer drug targeting hypoxia-inducible factor 1. *J Natl Cancer Inst* **95:**516–525.

Yeo EJ, Chun YS, and Park JW (2004) New anticancer strategies targeting HIF-1. *Biochem Pharmacol* **68:**1061–1069.

Address correspondence to: Wen-Mei Fu, Department of pharmacology, College of Medicine, National Taiwan University, 1, Sec. 1, Jen-Ai Road, Taipei, Taiwan., E-mail: wenmei@ntu.edu.tw